

theory developed here and in SP with which the experiments give qualitative verification is entirely based on the assumption that in the presence of a magnetic field, the Hamiltonian for the surface-state levels is given by the replacement

$$\vec{P} \rightarrow \vec{P} - e\vec{A}/c, \quad (18)$$

where \vec{A} is the vector potential. The results ob-

tained here indicate that this approximation remains valid when cubic terms are involved in the band structure.

ACKNOWLEDGMENTS

The authors wish to thank Professor A. K. Rajagopal for many helpful discussions.

*Work supported in part by the National Science Foundation, under grant No. GP-28730.

†Work performed at Louisiana State University while participating in the National Science Foundation Summer Research Participation for College Teachers Program.

¹S. P. Singhal and R. E. Prange, Phys. Rev. B 3, 4083 (1971) (the same notation is used throughout).

²R. A. Herrod, C. A. Gage, and R. G. Goodrich, Phys. Rev. B 4, 1033 (1971).

PHYSICAL REVIEW B

VOLUME 5, NUMBER 4

15 FEBRUARY 1972

Anharmonic Lattice Dynamics in Na

H. R. Glyde

*Atomic Energy of Canada Limited, Chalk River Nuclear Laboratories,
Chalk River, Ontario, Canada*

and

Roger Taylor

National Research Council, KLA OR6, Ottawa, Ontario, Canada

(Received 16 August 1971)

The phonon frequencies and lifetimes in Na at $T=5, 90, 160, 293,$ and 361°K have been computed employing both the self-consistent (SC) and perturbation theories of anharmonic-lattice dynamics. To describe Na an effective ion-ion potential derived from the calculations of Geldart *et al.* which employs the Geldart-Taylor screening function was used. For all the symmetry directions the computed frequencies were in excellent agreement with the observed values at both 90 and 293°K . The predicted lifetimes, however, did not agree so well, suggesting higher-anharmonic damping effects may be important. Comparison of the SC and perturbation results suggest that the frequency shifts are reduced in the SC theory, that the SC theory agrees marginally better with experiment, but that there is little to choose between the two for Na. The agreement with experiment suggests that Na can be well described by an effective two-body potential.

I. INTRODUCTION

Since the pioneering study of Toya¹ in 1958, many calculations of the lattice dynamics in Na have appeared. These have used various force-constant, pseudopotential, and orthogonalized-plane-wave (OPW) models with most incorporating fitting procedures to solid data to fix the potential parameters. All these calculations were made within the harmonic approximation with many achieving very good agreement with the observed phonon-dispersion curves at 90°K of Woods *et al.*² This work on sodium and the potentials are discussed in detail in the review article by Joshi and Rajagopal³ and by Price *et al.*⁴ to which the interested reader is referred.

In this paper we specifically study the anhar-

monic contribution to the lattice dynamics in Na to discuss three questions. First, by comparing the anharmonic and quasiharmonic (QH) results we may isolate the magnitude of anharmonic contributions, particularly at high temperature. Second, by computing the anharmonic contributions in both the self-consistent (SC) and standard perturbation theories of lattice dynamics, we may compare these two theories for a simple metal and estimate the sophistication needed to treat Na satisfactorily. Finally, by comparing with experiment we may test the validity of both the anharmonic theory and the fundamental interatomic potential which we use. A similar study of K, but employing a pseudopotential obtained by fitting to phonon-dispersion curves and a perturbation treatment of anharmonicity, has been made by

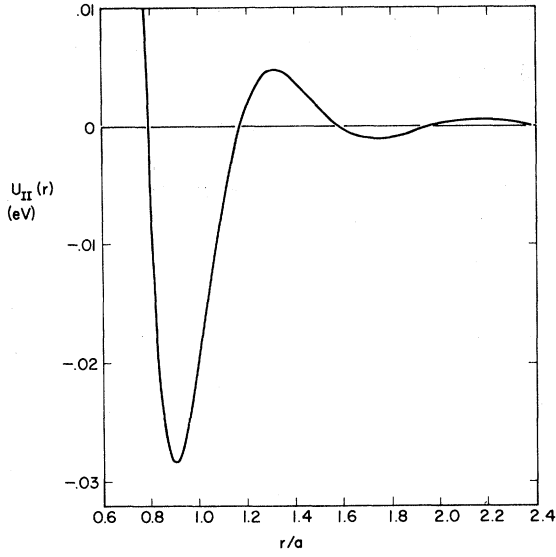


FIG. 1. 90°K effective ion-ion potential in Na as a function of the ion-ion separation in units of lattice parameter $a = 4.234 \text{ \AA}$.

Buyers and Cowley.⁵

II. EFFECTIVE ION-ION POTENTIAL

For the present calculation we have chosen the ion-ion potential derived from the calculation of Geldart *et al.*⁶ and discussed by Duesbery and Taylor⁷ and Basinski *et al.*⁸ For this potential the bare electron-ion interaction was calculated using a single OPW for the conduction-electron wave function which interacted with the Na^+ ion via the empirical Prokofjew⁹ potential. The Prokofjew electron- Na^+ potential was constructed to reproduce the spectroscopic-term values of the isolated ion. The choice of electron-gas screening for this problem is quite critical^{6,7} and we have used the Geldart-Taylor¹⁰ calculation of the dielectric function since, on comparison¹¹ with other functions, it appears to be the best one available. There are then no adjustable parameters to fit to solid data. Hence in view of the fundamental nature of the calculation and the excellent agreement with experimental lattice-dynamic data at 90°K obtained by Geldart *et al.*⁶ and Basinski *et al.*,⁸ this potential seems a suitable choice for anharmonic calculations. There are, of course, other ion-ion potentials calculated for Na, the most noteworthy of which is perhaps the calculation of Shyu *et al.*¹²

The extension of the potential calculation for the higher temperatures considered here is made simply by using the Na density appropriate to these temperatures. The calculations of Geldart *et al.*⁶ were then repeated at these densities. A typical potential is shown in Fig. 1.

III. ANHARMONIC THEORY

The SC theory of lattice dynamics¹³⁻¹⁸ has been discussed and reviewed^{13,16,19} by many authors and we outline below only those parts which are specifically used here. Starting with the usual QH theory, the lowest-order self-consistent harmonic (SCH) theory can be derived by retaining all the anharmonic terms which appear in the first-order anharmonic perturbation correction to the QH frequencies. These are all even anharmonic terms; the fourth-order term V_4 , the sixth-order term V_6 , and so on ($V_4 + V_6 + V_8 + \dots$). The summation of these contributions into closed form yields the expression for the SCH frequencies. This summation is represented graphically in Fig. 2 and the closed expression for the SCH frequency (Ω_{qj}) for phonon with wave vector \vec{q} and branch j is

$$\Omega_{qj}^2 = \frac{1}{M} \sum_{l \neq l'} (e^{i\vec{q} \cdot \vec{R}(ll')} - 1) \sum_{\alpha\beta} \epsilon_{qj}^\alpha \epsilon_{qj}^\beta \left\langle \frac{\partial^2 v(\vec{r}(ll'))}{\partial r_\alpha(l) \partial r_\beta(l')} \right\rangle, \quad (1)$$

where $\vec{R}(ll')$ is a lattice vector, ϵ_{qj}^α is the α component of a polarization vector and $v(\vec{r}(ll'))$ is the effective ion-ion potential. The expectation value in (1) can be written as a space integral^{14,17} in the difference coordinate $u \equiv \vec{r}(ll') - \vec{R}(ll')$ as

$$\left\langle \frac{\partial^2 v}{\partial r_\alpha \partial r_\beta} \right\rangle = [(2\pi)^3 |\bar{\Lambda}|]^{-1/2} \int d\vec{u} e^{-i(\vec{q}/2) \cdot \vec{u}} \bar{\Lambda}^{-1} \cdot \vec{u} \frac{\partial^2 v}{\partial r_\alpha \partial r_\beta}, \quad (2)$$

where

$$\Lambda_{\alpha\beta}(ll') = \frac{h}{NM} \sum_{qj} (1 - e^{i\vec{q} \cdot \vec{R}(ll')}) \epsilon_{qj}^\alpha \epsilon_{qj}^\beta \frac{\coth(\frac{1}{2}\beta\hbar\Omega_{qj})}{\Omega_{qj}} \quad (3)$$

and $\beta = 1/kT$. Since $\bar{\Lambda}(ll')$ depends on Ω_{qj} , (1)-(3) must be solved iteratively to obtain the final SCH frequencies.

If, however, the QH frequencies ω_{qj} are substituted into (3) and the resulting $\bar{\Lambda}(ll')$ is used directly to compute the expectation value, then the frequencies obtained from (1) are the QH

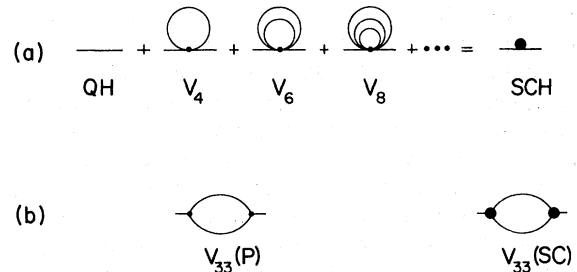


FIG. 2. (a) QH frequency plus the even anharmonic terms appearing in the first-order correction which are summed to obtain the SCH frequency expression; (b) cubic anharmonic term as computed in the QH and SCH basis.

frequencies plus a perturbative shift $\Delta\nu_1$ (PT) due to the anharmonic terms; $V_4 + V_6 + \dots$.²⁰ Employing (1)–(3) with a prior calculation of the QH frequencies in this way, we may thus compute the frequency shift $\Delta\nu_1$ (PT) due to those anharmonic terms which appear in the SCH theory as they would be calculated in a standard perturbation theory.²¹

The leading correction to the SCH frequencies is the cubic anharmonic term.^{16,22} The frequency of phonon $qj = \lambda$ with this cubic term added as a perturbation is then identified with the peak in the response function:

$$\left(\frac{2\omega_{qj} \Gamma(\omega)}{[-\omega^2 + \Omega_{qj}^2 + 2\Omega_{qj} \Delta(\omega)]^2 + [2\Omega_{qj} \Gamma(\omega)]^2} \right) \times \frac{1}{2\pi} (1 - e^{-\beta\hbar\omega})^{-1}, \quad (4)$$

where

$$\Delta(\lambda, \omega) = -\frac{1}{2\hbar^2} \sum_{\lambda_1 \lambda_2} |\langle V(\lambda, \lambda_1 \lambda_2) \rangle|^2 \times \left(\frac{n_1 + n_2 + 1}{(\Omega_1 + \Omega_2 + \omega)_p} + \frac{n_1 + n_2 + 1}{(\Omega_1 + \Omega_2 - \omega)_p} + \frac{n_2 - n_1}{(\Omega_1 - \Omega_2 + \omega)_p} + \frac{n_2 - n_1}{(\Omega_1 - \Omega_2 - \omega)_p} \right) \quad (5)$$

and

$$\Gamma(\lambda, \omega) = \frac{\pi}{2\hbar^2} \sum_{\lambda_1 \lambda_2} |\langle V(\lambda, \lambda_1, \lambda_2) \rangle|^2 \{ (n_1 + n_2 + 1) \times [\delta(\Omega_1 + \Omega_2 - \omega) - \delta(\Omega_1 + \Omega_2 + \omega)] + (n_2 - n_1) [\delta(\Omega_1 - \Omega_2 - \omega) - \delta(\Omega_1 - \Omega_2 + \omega)] \} \quad (6)$$

are the real and imaginary parts of the self-energy due to the cubic term, respectively; $\Omega_i = \Omega_{\lambda_i}$ are the SCH frequencies, $n_i = (e^{\beta\hbar\Omega_i} - 1)^{-1}$, and $V(\lambda, \lambda_1, \lambda_2)$ is the cubic-potential coefficient [see Eq. (8) of Ref. 20]. The representations $1/(x)_p = x/(x^2 + \epsilon^2)$ and $\pi\delta(x) = \epsilon/(x^2 + \epsilon^2)$ were used for the principal part and δ functions. With the cubic term included, the resulting frequencies are denoted here as SCH+C. The frequency shift due to the cubic term, $\Delta_{33}(\text{SC})$, is defined here as the difference between the peak in (4) and the SCH frequency.

In standard perturbation theory,²¹ the correction to the QH frequencies for the cubic term is identical to (4)–(6) except that $\langle V(\lambda, \lambda_1, \lambda_2) \rangle$ is replaced by $V(\lambda, \lambda_1, \lambda_2)$ and the QH ω_{qj} replace the SCH Ω_{qj} everywhere. Also, in the denominator of (4) we must include the shift due to the first-order terms. Making these changes the cubic shift in standard perturbation theory, $\Delta\nu_{33}(\text{PT})$, defined here as the difference between the frequency QH + $\Delta\nu_1(\text{PT})$ and the peak in (4), may

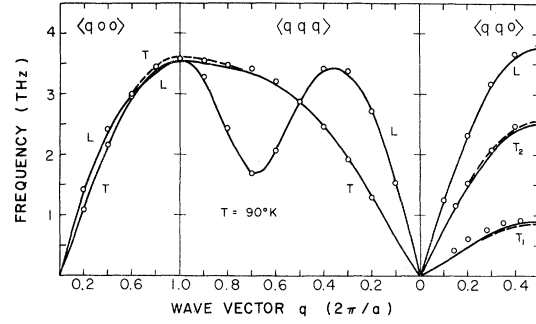


FIG. 3. Phonon-frequency dispersion curves in Na at $T = 90^\circ\text{K}$: solid line, SCH+C; dashed line, QH. The circles are the observed values of Woods *et al.*

be computed.

IV. NUMERICAL RESULTS

A. SC Theory and Comparison with Experiment

1. Phonon Frequencies

The phonon-frequency-dispersion curves computed in the SCH+C and QH approximations at $T = 90^\circ\text{K}$ are shown in Fig. 3. From Fig. 3 anharmonic effects are clearly small at 90°K and both approximations compare equally well with the experimental values of Woods *et al.* The same dispersion curves at $T = 293^\circ\text{K}$ are shown in Fig. 4 along with the experimental data of Millington and Squires.²³ There, anharmonic effects are important and the SCH+C approximation compares much better with experiment. The net shifts in frequency due to anharmonic effects are most pronounced near the $(1, 0, 0)$ point and along the two transverse branches in the $[110]$ direction.

Figure 5 shows the SCH and SCH+C approximations for the $\langle 110 \rangle$ direction at 293°K . The difference between these two curves represents the shift due to the cubic anharmonic term $\Delta\nu_{33}(\text{S})$. Comparing Figs. 4 and 5 we see that (a) for the longitudinal (L) $\langle 110 \rangle$ branch the shift from the QH to the SCH case is essentially cancelled by the cubic shift so that the QH and SCH+C values are nearly equal; (b) for the transverse T_2 $\langle 110 \rangle$ branch the QH to SCH shift and the cubic shift are both downward with the cubic shift being much larger; and (c) for the transverse T_1 $\langle 110 \rangle$ branch the QH to SCH shift is about twice the cubic shift. As a result of the large first-order shift, the temperature dependence of the T_1 $\langle 110 \rangle$ phonon frequencies differ in sign for the QH and SCH+C cases with the latter agreeing with experiment at 293°K . Hence, to get agreement with experiment for the T_1 $\langle 110 \rangle$ branch at both 90 and 293°K , anharmonic contributions are crucial. The phonon frequencies for the $\langle 110 \rangle$ directions and $(1, 0, 0)$ and $(0.5, 0.5, 0.5)$ points are listed in detail in

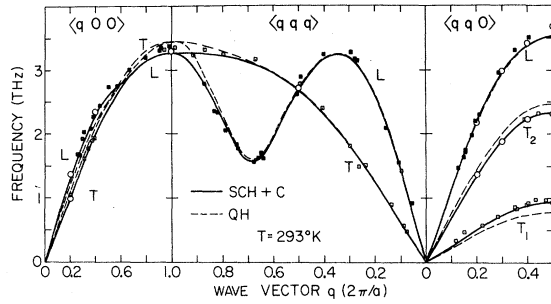


FIG. 4. Phonon-frequency dispersion curves in Na at 293°K: solid line, SCH+C; dashed line, QH. The open squares are the transverse and the solid squares the longitudinal observed values of Millington and Squires. The open circles are the observed values of Woods *et al.*, Brockhouse *et al.*, Woods, and some unpublished Chalk River results.

Tables I and II. Also listed are some observed results taken from Woods *et al.*,^{2,24} Woods,²⁵ Brockhouse *et al.*,^{26,27} and unpublished Chalk River data. The estimated error on the observed points is 2–3%.

The elastic constants and bulk modulus obtained from the long-wavelength limit of the SCH+C phonon-dispersion curves are listed in Table III. They have been summed over 19 neighbors only and not to complete convergence as discussed by Basinski *et al.*⁸

2. Phonon Group Widths

The phonon group, as given by Eq. (4), for the $T_1(0.5, 0.5, 0)$ phonon is shown in Fig. 6 for five temperatures from $T = 5^\circ\text{K}$ to 361°K . The full width at half-height $W \approx 2\Gamma$ of this group was as large as any other phonon group, which is unusual for a relatively low-frequency phonon. Since

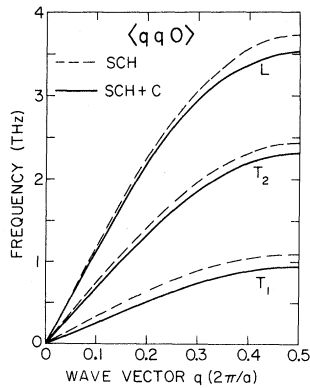


FIG. 5. Phonon-frequency dispersion curves along the $\langle q q 0 \rangle$ direction for the SCH and SCH+C approximations in Na at 293°K. The difference between these two curves represents the frequency shift due to the cubic anharmonic term $\Delta\nu_{33}$ (SC).

TABLE I. Temperature dependence of the phonon frequencies (in 10^{12} Hz) for the $[q, q, 0]$ direction in Na as observed (obs) (see text) and computed in the QH, SCH, and SCH+C approximations. W is the computed phonon group width at half-height (in 10^{12} Hz).

q		Temperature ($^\circ\text{K}$)					
		5	90	160	215	296	361
L							
0.2	obs		2.32		2.24	2.16	
	QH	2.320	2.305	2.262		2.177	2.135
	SCH	2.345	2.335	2.316		2.264	2.242
	SCH+C	2.32	2.30	2.27		2.19	2.15
	W	0.004	0.020	0.027		0.044	0.069
0.3	obs		3.17		3.05	2.98	
	QH	3.150	3.121	3.061		2.933	2.867
	SCH	3.184	3.170	3.140		3.073	3.041
	SCH+C	3.14	3.12	3.07		2.94	2.89
	W	0.013	0.036	0.064		0.100	0.109
0.4	obs		3.67		3.50	3.41	
	QH	3.628	3.594	3.520		3.369	3.283
	SCH	3.671	3.660	3.627		3.557	3.516
	SCH+C	3.62	3.59	2.52		3.37	3.31
	W	0.022	0.049	0.078		0.12	0.14
0.5	obs		3.82		3.71	3.68	
	QH	3.795	3.758	3.680		3.522	3.426
	SCH	3.842	3.829	3.796		3.724	3.680
	SCH+C	3.79	3.77	3.68		3.53	3.45
	W	0.029	0.070	0.13		0.17	0.22
T_1							
0.2	obs					0.442	0.451
	QH	0.462	0.472	0.454		0.644	0.664
	SCH	0.493	0.552	0.594		0.51	0.51
	SCH+C	0.48	0.49	0.50		0.16	0.08
	W	0.0001	0.045	0.084			
0.3	obs					0.626	0.629
	QH	0.672	0.682	0.659		0.890	0.918
	SCH	0.705	0.778	0.827		0.73	0.74
	SCH+C	0.69	0.71	0.72		0.26	0.12
	W	0.0005	0.079	0.14			
0.4	obs					0.739	0.738
	QH	0.802	0.812	0.783		1.044	1.077
	SCH	0.837	0.918	0.972		0.89	0.91
	SCH+C	0.82	0.85	0.87		0.31	0.15
	W	0.0008	0.1	0.16			
0.5	obs		0.93		0.93	0.93	
	QH	0.845	0.855	0.824		0.777	0.776
	SCH	0.881	0.966	1.022		1.097	1.132
	SCH+C	0.86	0.89	0.93		0.95	0.97
	W	0.001	0.10	0.17		0.28	0.23
T_2							
0.2	obs		1.52		1.43	1.37	
	QH	1.499	1.498	1.480		1.453	1.446
	SCH	1.503	1.490	1.474		1.432	1.423
	SCH+C	1.49	1.46	1.43		1.35	1.33
	W	0.0007	0.029	0.54		0.10	0.13
0.3	obs		2.09		1.96	1.88	
	QH	2.079	2.070	2.048		2.006	1.995
	SCH	2.083	2.060	2.034		1.974	1.961
	SCH+C	2.06	2.02	1.98		1.89	1.86
	W	0.003	0.036	0.070		0.11	0.14
0.4	obs		2.47		2.34	2.23	
	QH	2.446	2.434	2.407		2.357	2.344
	SCH	2.451	2.424	2.391		2.320	2.303
	SCH+C	2.43	2.39	2.34		2.23	2.20
	W	0.006	0.035	0.065		0.10	0.15
0.5	obs		2.56		2.45	2.31	
	QH	2.572	2.559	2.529		2.476	2.464
	SCH	2.576	2.548	2.513		2.439	2.421
	SCH+C	2.56	2.51	2.46		2.33	2.31
	W	0.006	0.040	0.087		0.11	0.12

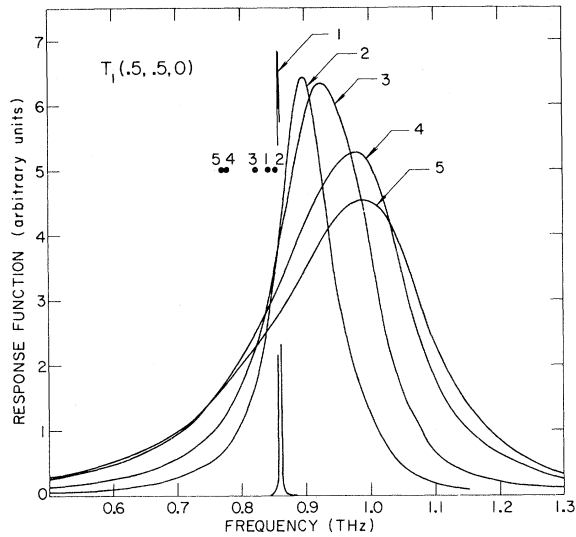


FIG. 6. Phonon group or scattering-response function for the $T_1(0.5, 0.5, 0)$ phonon as a function of temperature; 1, 5°K; 2, 90°K; 3, 160°K; 4, 296°K; and 5, 361°K. The solid dots show the values of the QH harmonic frequencies at the five temperatures.

$T_1(0.5, 0.5, 0)$ has a relatively low frequency, the predominant contribution to Γ must come from the last two terms in Eq. (6). The large width thus suggests there is an unusually large density of phonons arranged so that $\Omega_1 - \Omega_2 \pm$ is often nearly zero for ω approximately equal to the frequency of the $T_1(0.6, 0.5, 0)$ phonon. Phonon groups for the $(1, 0, 0)$ and $L(0.5, 0.5, 0)$ phonons are shown in Fig. 7. These and Fig. 6 are typical of all the phonon groups and no unusual peak shapes or doubly peaked groups were found.

In Fig. 8, the width W computed for the $T_2(q, q, 0)$ phonon groups are shown and compared with the observed W of Woods. The comparison shows clearly that the computed width for this branch is much too small—as much as a factor of 3 at

TABLE II. Temperature dependence of the phonon frequencies (in 10^{12} Hz) for the $q = (0.5, 0.5, 0.5)$ and $(1, 0, 0)$ phonons in Na as observed (obs) and computed in the QH, SCH, and SCH+C approximations. W is the computed phonon group width in 10^{12} Hz.

Phonon	Approx.	Temperature (°K)					
		5	90	160	215	296	361
$(0.5, 0.5, 0.5)$	obs		2.88		2.82	2.72	
	QH	2.877	2.852	2.795		2.680	2.632
	SCH	2.910	2.909	2.892		2.846	2.830
	SCH+C	2.87	2.86	2.82		2.70	2.64
	W	0.015	0.046	0.076		0.099	0.18
$(1, 0, 0)$	obs		3.58		3.41	3.29	
	QH	3.644	3.613	3.557		3.450	3.414
	SCH	3.663	3.631	3.585		3.489	3.463
	SCH+C	3.61	3.54	3.45		3.26	3.20
	W	0.020	0.032	0.060		0.053	0.77

TABLE III. Elastic constants (in 10^{10} /dyne/cm²) in Na as computed from the long-wavelength limit of the SCH + C phonon-dispersion curves. B is the bulk modulus, $B = \frac{1}{3}(c_{11} + 2c_{12})$.

T	c_{11}	c_{12}	c_{44}	$\frac{1}{2}(c_{11} - c_{12})$	B
5	7.89	7.01	5.44	0.447	7.30
90	7.90	6.96	5.25	0.470	7.27
160	7.84	6.78	4.97	0.531	7.13
293	7.51	6.48	4.14	0.519	6.82
361	7.00	5.96	4.12	0.519	6.31

large q . A similar discrepancy was found by Buyers and Cowley⁵ and this is discussed in Sec. V.

B. Comparison of SC and Perturbative Treatments

The frequency shifts due to anharmonic terms as calculated in the SC and standard perturbation theories for the $q = (0.5, 0.5, 0)$ phonon are listed in Table IV as a function of temperature. A similar comparison for the $T_1[q, q, 0]$ branch at $T = 361^\circ\text{K}$ is made in Table V. In these tables $\Delta\nu_1(\text{PT})$ is the size of the frequency shift due to the anharmonic terms V_4, V_6, V_8, \dots when they are treated as simple perturbations to the QH theory. $\Delta\nu_1(\text{SC}) \equiv \Omega(\text{SCH}) - \Omega(\text{QH})$ represents the size of these terms when evaluated in the SCH basis. $\Delta\nu_{33}(\text{SC})$ and $\Delta\nu_{33}(\text{PT})$ are the sizes of the cubic shift when it is evaluated in the SC and perturbative methods, respectively. The exact definition of each shift is given in Sec. II.

From Table IV we see that both shifts are nearly always reduced when evaluated in the SCH basis. This is particularly true for $\Delta\nu_1$. From this point of view the SCH basis can be regarded as an improvement since subsequent corrections to it are small. The difference, however, is of significance only for room temperature and above and then really only for the $T_1[q, q, 0]$ branch. For this branch $\Delta\nu_1$ is reduced by $\sim 25\%$ in the SCH

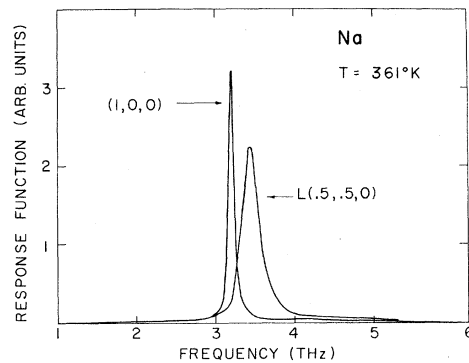


FIG. 7. Phonon groups for the $L(0.5, 0.5, 0)$ and $(1, 0, 0)$ phonons at $T = 361^\circ\text{K}$.

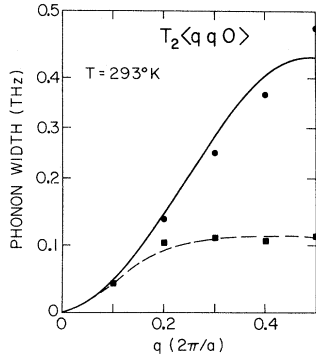


FIG. 8. Group width W for the $T_2 \langle q, q, 0 \rangle$ phonons at $T = 296^\circ\text{K}$. The circles and solid line are the observed values of Woods. The squares and dashed line are the values computed here in the SCH+C approximation.

basis. Also, since $\Delta\nu_1 \sim 0.6\Omega_{\text{QH}}$ for this branch, the SC theory can be regarded as an improvement since this large term is incorporated in the zero order in the SC theory while it remains a correction in the perturbation method. This last argument cannot be generalized to any crystal or any branch and will certainly not be convincing if $\Delta\nu_{33} \gtrsim \Delta\nu_1$.

The perturbation frequency is defined here as the QH frequency plus a perturbative evaluation of $V_4 + V_6 + V_8 + \dots$ to first order and the cubic term to second order, $\Omega(\text{PT}) \equiv \Omega(\text{QH}) + \Delta\nu_1(\text{PT}) + \Delta\nu_{33}(\text{PT})$. It should not be confused with the usual anharmonic-perturbation frequencies which normally include only V_4 to first order and the cubic term as treated here. The first-order shift then would not be so large. From Tables IV and

V we see that the perturbation and SCH+C values do differ somewhat. For the $L(0.5, 0.5, 0)$ and $T_2(0.5, 0.5, 0)$ phonons this difference would be increased if only V_4 were included and from Fig. 4 the SCH+C values agree better with experiment. The largest difference is for the $T_1[q, q, 0]$ branch where the perturbation values lie $\sim 10\%$ above the SCH+C values. Here, however, including only V_4 in perturbation theory would tend to bring the two cases together. In summary, a perturbation treatment such as that of Buyers and Cowley⁵ using the present QH frequencies would give substantially the same results as the SCH+C approximation with the two differing by at most $\sim 5\%$. Where these differences occur the SCH+C values appear to agree best with experiment.

V. DISCUSSION AND CONCLUSION

The results of Sec. IV show that anharmonic effects are clearly important in Na at room temperature and upwards. The net shifts in phonon frequency are most pronounced around the $(1, 0, 0)$ point and along the two transverse branches in the $[110]$ direction. The shift is downward for the $T_2[q, q, 0]$ branch and upward for the $T_1[q, q, 0]$ branch so that the separation between the two branches and hence the crystal anisotropy is considerably reduced in the SCH+C case. For this reason a QH theory employing a realistic potential could not hope to fit the observed dispersion curves closely at room temperature. If a fit were obtained, the potential would have to simulate the anharmonic contributions in some way. The anharmonic contributions also predict a pronounced flattening of the $L[q, 0, 0]$ branch at large q which agrees with the shape observed by

TABLE IV. Frequencies, shifts, and widths (in THz) computed for the $[0.5, 0.5, 0]$ phonon in Na employing the perturbative (PT) and self-consistent (SC) methods as a function of temperature. QH: quasiharmonic frequencies; SCH: self-consistent harmonic frequencies; QH+ $\Delta\nu_1(P)$: QH plus perturbative evaluation of the terms $V_4 + V_6 + V_8 + \dots$ which are included in the SCH case; SCH+C: SCH plus self-consistent evaluation of the cubic term; PT: QH+ $\Delta\nu_1(\text{PT}) + \Delta\nu_{33}(\text{PT})$; $\Delta\nu_1(\text{PT})$, $\Delta\nu_1(\text{SC})$: frequency shift due to $V_4 + V_6 + V_8 + \dots$ in perturbation and SC cases, respectively; $\Delta\nu_{33}(\text{PT})$, $\Delta\nu_{33}(\text{SC})$: frequency shift due to the cubic term in the perturbation and SC cases, respectively. $W(\text{PT})$, $W(\text{SC})$: scattering response width in PT and SC cases.

Branch	Temp. (°K)	QH	SCH	QH+ $\Delta\nu_1(P)$	SCH+C	PT	$\Delta\nu_1(\text{PT})$	$\Delta\nu_1(\text{SC})$	$\Delta\nu_{33}(\text{PT})$	$\Delta\nu_{33}(\text{SC})$	$W(\text{PT})$	$W(\text{SC})$
L	90	3.758	3.829	3.831	3.77	3.74	+0.073	+0.071	-0.09	-0.06	0.08	0.07
	160	3.680	3.796	3.801	3.68	3.66	+0.121	+0.116	-0.14	-0.12	0.14	0.13
	293	3.522	3.724	3.744	3.53	3.48	+0.222	+0.202	-0.26	-0.20	0.25	0.17
	361	3.426	3.680	3.708	3.45	3.37	+0.282	+0.254	-0.34	-0.23	0.29	0.22
T_2	90	2.559	2.548	2.545	2.51	2.51	-0.014	-0.011	-0.05	-0.04	0.05	0.04
	160	2.529	2.513	2.500	2.46	2.44	-0.029	-0.016	-0.06	-0.06	0.09	0.09
	293	2.476	2.439	2.404	2.33	2.31	-0.072	-0.037	-0.09	-0.11	0.22	0.11
	361	2.464	2.421	2.378	2.31	2.25	-0.086	-0.043	-0.13	-0.12	0.28	0.12
T_1	90	0.885	0.996	0.984	0.89	0.89	+0.129	+0.110	-0.09	-0.08	0.13	0.10
	160	0.824	1.022	1.068	0.93	0.94	+0.244	+0.198	-0.13	-0.09	0.30	0.17
	293	0.777	1.097	1.219	0.95	1.06	+0.442	+0.320	-0.16	-0.16	0.15	0.28
	361	0.776	1.132	1.274	0.97	1.08	+0.498	+0.356	-0.20	-0.16	0.20	0.23

TABLE V. Comparison of the perturbative (PT) and self-consistent (SC) shifts and width (in THz) for the $T_1 [q, q, 0]$ phonon at $T=361^\circ\text{K}$. The notation is explained in Table IV.

q	QH	SCH	QH + $\Delta\nu_1(P)$	SCH + C	PT	$\Delta\nu_1(\text{PT})$	$\Delta\nu_1(\text{SC})$	$\Delta\nu_{33}(\text{PT})$	$\Delta\nu_{33}(\text{SC})$	$W(\text{PT})$	$W(\text{SC})$
0.5	0.776	1.132	1.274	0.97	1.08	+0.498	+0.356	-0.20	-0.16	0.20	0.23
0.4	0.738	1.077	1.211	0.91	1.00	+0.473	+0.339	-0.21	-0.17	0.27	0.15
0.3	0.629	0.918	1.029	0.74	0.78	+0.400	+0.289	-0.25	-0.17	0.45	0.11
0.2	0.451	0.664	0.744	0.51	0.48	+0.293	+0.214	-0.26	-0.15	0.22	0.08
0.1	0.225	0.344	0.386	0.25	0.21	+0.161	+0.119	-0.18	-0.10	0.09	0.06

Millington and Squires.²³ Koehler²² has predicted a similar flattening of this branch in solid Ne due to anharmonicity.

Since the SCH + C dispersion curves in Figs. 3 and 4 broadly agree very well with the observed curves, further anharmonic or many-body potential contributions not included here are either reasonably small or such that their contributions to the frequency shifts largely cancel. The work of Shukla and Cowley²⁸ on the thermodynamic properties of alkali halides suggests that the latter is possible although one would not expect this to be true for each branch. Figure 3 and 4 do suggest however, that there may be some discrepancy outside the experimental error near the (1, 0, 0) point and along the $T_1\langle 110 \rangle$ branch. Since these are the areas, particularly $T_1\langle 110 \rangle$, which are most sensitive to anharmonic effects, these differences suggest some small further anharmonic contributions. The additional terms included by Goldman *et al.*,²⁹ for example, are of the correct sign and approximate magnitude to improve the agreement.

The comparison of the anharmonic contributions computed in the SC theory and standard perturbation theory shows that these contributions are reduced in the SC method, particularly when their contribution is large. From this point of view the SC method can be regarded as an improvement on the perturbation treatment. However, since a perturbation treatment of the quartic and cubic terms combined with the present QH theory would give nearly as good final results as the SCH + C case here, there is not much to choose between the two from an operational point of view in Na. This differs from the situation in rare-gas crystals where perturbation treatments³⁰ appear to break down completely at higher temperatures.

The present results can be most closely compared with those of Buyers and Cowley⁵ in K. They employed a pseudopotential, with parameters determined by fits to the observed dispersion curves at 9°K and the elastic constants, together with a perturbative calculation of the quartic and cubic terms. They found explicit anharmonic frequency shifts of essentially the same size and variations throughout the Brillouin zone as found here. In particular, the quartic shift for the

$T_1(0.5, 0.5, 0)$ phonon was also $\sim 60\%$ of the QH frequency in K which, since this is the same size as the shift $\Delta\nu_1(\text{PT})$ here, suggests that nearly all of $\Delta\nu_1(\text{PT})$ is due to the quartic term. The most significant difference occurred in the treatment of the thermal or expansion shifts appearing in the QH approximation. For the $L\langle 111 \rangle$ branch the downward shift in the QH frequency was much greater here and apparently in much better agreement with experiment. It is difficult to say whether this is due to the more exact QH theory employed here or to a difference in the screening appearing in the potential. Since Millington and Squires used the more exact QH theory and a fitted screening function similar to Buyers and Cowley and also computed a $L\langle 111 \rangle$ branch giving larger frequencies than observed, the difference here may well be due to an improved potential.

The computed phonon group widths were generally much less than the observed ones. This discrepancy, in the same direction and size, also occurred in the calculations of Buyers and Cowley who discuss a number of phonon damping contributions which have not been included in either calculation. Of these contributions, higher-order anharmonicity and one-phonon or two-phonon interference or multiphonon contributions to the scattering cross section appear the most probable to us. However, we are not able to add anything more concrete to the explanations of Buyers and Cowley and this remains a significant disagreement with experiment.

Millington and Squires have computed dispersion curves for Na at room temperature within the QH approximation and employing a fitted pseudopotential. Their computed dispersion curves differ from their observed points, most along the $\langle qq q \rangle$ direction at large q , the $L\langle q, q, 0 \rangle$ at high q and along $T_1\langle q, q, 0 \rangle$. Comparing with the present results, the discrepancy along $T_1\langle q, q, 0 \rangle$ is almost certainly due to anharmonic effects. For the $\langle q, q, q \rangle$ at large q , the discrepancy is probably a complicated combination of anharmonicity and their particular choice of screening. For $L\langle q, q, 0 \rangle$ it is most probably a screening effect. Geldart *et al.* have discussed in detail the dependence of the dispersion curves on screening and their re-

sults suggest that a Hubbard screening model would provide dispersion curves which are generally too high at large- q values.

In conclusion then, the present results show that with a careful choice of dielectric function and including anharmonic effects, good agreement with experimental dispersion curves at $T=90^\circ\text{K}$ and room temperature can be obtained without

prior fitting to solid data.

ACKNOWLEDGMENTS

We are grateful to Dr. A. D. B Woods and Professor B. N. Brockhouse for valuable discussion of this subject and for permission to quote some unpublished data appearing in Tables I and II.

-
- ¹T. Toya, J. Res. Inst. Catalysis, Hokkaido Univ. 6, 161 (1958); 6, 183 (1958).
- ²A. D. B. Woods, B. N. Brockhouse, R. H. March, A. T. Stewart, and R. Bowers, Phys. Rev. 128, 1112 (1962).
- ³S. K. Joshi and A. K. Rajagopal, Solid State Phys. 22, 159 (1968).
- ⁴D. L. Price, K. S. Singwi, and M. P. Tosi, Phys. Rev. B 2, 2983 (1970).
- ⁵W. J. L. Buyers and R. A. Cowley, Phys. Rev. 180, 755 (1969).
- ⁶D. J. W. Geldart, R. Taylor, and Y. P. Varshni, Can. J. Phys. 48, 183 (1970).
- ⁷M. S. Duesbery and R. Taylor, Phys. Letters 30A, 496 (1969).
- ⁸Z. S. Basinski, M. S. Duesbery, A. P. Pogany, R. Taylor, and Y. P. Varshni, Can. J. Phys. 48, 1480 (1970).
- ⁹E. P. Wigner and F. Seitz, Phys. Rev. 43, 804 (1933).
- ¹⁰D. J. W. Geldart and R. Taylor, Can. J. Phys. 48, 167 (1970).
- ¹¹D. J. W. Geldart and R. Taylor, Solid State Commun. 9, 7 (1971).
- ¹²W. M. Shyu, K. S. Singwi, and M. P. Tosi, Phys. Rev. B 3, 237 (1971).
- ¹³P. F. Choquard, *The Anharmonic Crystal* (Benjamin, New York, 1967).
- ¹⁴N. Boccara and G. Sarma, Physics 1, 219 (1965).
- ¹⁵T. R. Koehler, Phys. Rev. Letters 17, 89 (1966).
- ¹⁶H. Horner, Z. Physik 205, 72 (1967).
- ¹⁷N. S. Gillis, N. R. Werthamer, and T. R. Koehler, Phys. Rev. 165, 951 (1968).
- ¹⁸N. R. Werthamer, Am. J. Phys. 37, 763 (1969); Phys. Rev. B 1, 572 (1970).
- ¹⁹H. R. Glyde and M. L. Klein, Crit. Rev. Solid State Sci. 2, 181 (1971).
- ²⁰H. R. Glyde, Can. J. Phys. 49, 761 (1971).
- ²¹R. A. Cowley, Rept. Progr. Phys. 31, 123 (1968); Advan. Phys. 12, 421 (1963).
- ²²T. R. Koehler, Phys. Rev. Letters 22, 777 (1969).
- ²³A. J. Millington and G. L. Squires, J. Phys. F 1, 244 (1971).
- ²⁴A. D. B. Woods, B. N. Brockhouse, R. H. March, and R. Bowers, Bull. Am. Phys. Soc. 6, 261 (1961).
- ²⁵A. D. B. Woods, *Inelastic Scattering of Neutrons in Solids and Liquids* (IAEA, Vienna, 1962), p. 3.
- ²⁶B. N. Brockhouse, S. Hautecler, and H. Stiller, *Interaction of Radiation with Solids*, edited by R. Strumane, J. Nihoul, R. Gevers, and S. Amelinckx (North-Holland, Amsterdam, 1964), p. 560.
- ²⁷B. N. Brockhouse, A. D. B. Woods, G. Dolling, and I. M. Thorson, Atomic Energy of Canada Ltd. Report No. 2012, 1964 (unpublished).
- ²⁸R. C. Shukla and E. R. Cowley, Phys. Rev. B 3, 4055 (1971).
- ²⁹V. V. Goldman, G. K. Horton, and M. L. Klein, Phys. Rev. Letters 24, 1424 (1970).
- ³⁰M. L. Klein, G. K. Horton, and J. L. Feldman, Phys. Rev. 148, 968 (1969).